Core-level shifts for two- and three-dimensional bimetallic Pd_xCu_{1-x} and Pd_xAg_{1-x} alloys on Ru(0001)

W. Olovsson,[1] L. Bech,[2] T. H. Andersen,[3] Z. Li,[4] S. V. Hoffmann,[4] B. Johansson,[1,5] I. A. Abrikosov,[6] and J. Onsgaard[2]
[1]*Condensed Matter Theory Group, Department of Physics, Uppsala University, SE-751 21 Uppsala, Sweden*
[2]*Department of Physics and Nanotechnology, Aalborg University, DK-9220 Aalborg East, Denmark*
[3]*Department of Physics, Norwegian University of Science and Technology, N-7491 Trondheim, Norway*
[4]*Institute of Storage Ring Facilities, University of Aarhus, DK-8000 Aarhus C, Denmark*
[5]*Applied Materials Physics, Department of Materials Science and Engineering, Royal Institute of Technology, SE-100 44 Stockholm, Sweden*
[6]*Department of Physics and Measurement Technology, Linköping University, SE-581 83 Linköping, Sweden*
(Received 22 February 2005; revised manuscript received 20 June 2005; published 29 August 2005)

Core-level binding energy shifts (CLSs) and surface CLS (SCLSs) are determined by experiment and theory for ultrathin Pd as well as for PdCu and PdAg surface alloys which vary in thickness from 1 to 4 monolayers (MLs), supported on Ru(0001). Experimentally, the binding energies of Pd and Ag $3d_{5/2}$ are measured by photoelectron spectroscopy using synchrotron radiation, and in the case of Cu $2p_{3/2}$ by x rays (XPS) from a Mg K_α radiation source. The calculations are based on first-principles techniques together with the complete screening picture, including initial and final state effects directly in the same scheme. Dimensional as well as temperature effects are observed and reproduced theoretically, with a good agreement between the calculated CLS and the experimentally observed values. Further it is demonstrated how the layer composition profile of a 4 ML thick PdAg film can be followed by comparing theoretical layer specific CLSs with the measured ones and combine this with the observed intensities of the Ag $3d_{5/2}$ photoelectrons.

DOI: 10.1103/PhysRevB.72.075444 PACS number(s): 68.55.Jk, 71.15.−m, 79.60.Dp

I. INTRODUCTION

Synthesis and characterization of bimetallic alloys are of importance for a number of technological applications like for example catalysis, sensors on the microscopic scale, and electronics on the nanometerscale. Studies of the electronic and geometrical structures of ultrathin bimetallic films including Pd—Pd_xCu_{1-x} and Pd_xAg_{1-x}—are motivated by the need to obtain a better understanding of their alloying conditions, low-dimensional effects, and catalytic properties. Ultrathin bimetallic films can have electronic and geometrical structures which differ quite radically from those of the bulk structure, something that can substantially alter their electronic and chemical properties. These changes are reflected in the binding energies of the core electrons, as they are sensitive to the local chemical environment.

Photoelectron spectroscopy (PES) based on application of synchrotron radiation with the possibility of tuning the photon energy and standard x-ray sources in combination with high-resolution electron energy analyzers is well suited to study the electronic structures in the different layers via measurements of the binding energies, in this 0 to 1 nm thickness regime. Parallel to this experimental possibility, calculations of CLSs and SCLSs can be performed, where the geometrical structure of the overlayers, and even different compositions in the various layers, can be modeled.

The bulk CLSs over the whole composition range for the Cu $2p_{3/2}$, Pd and Ag $3d_{5/2}$ in the fcc random PdCu and PdAg alloys were recently calculated *ab initio* using the complete screening picture, which includes initial state (core-electron energy eigenvalue) and final state (screening of the core hole) effects in the same scheme.[1,2] Comparisons were made with experimental CLS results for PdCu (Refs. 3–5) and PdAg alloys,[6] in which the samples were prepared as disordered solid solutions by melting high purity component metals under an Ar ion arc furnace followed by rapid quenching, with homogeneity obtained by reorienting and remelting. The agreement between theory and experiment was found to be very good. An alternative way of producing bimetallic samples, and which is explored in this work, is to codeposit the two metals on a substrate where no interdiffusion between the components of the overlayer and the substrate takes place. Hereby ultrathin films, surface alloys, can be produced. A possible consequence of this synthesis of two metals "from bottom up" is that the structure of the film may vary in the first few layers (numbered from the interface between the surface of the substrate and the first layer) through the next bulk layer(s), and the surface layer of the film. Thus, the properties of three-layer thick films can differ due to different coordination numbers in the layers.

The "bottom up" principle used in the formation of the films makes it possible to follow low-dimensional effects in the first overlayer, which is in fact two-dimensional, provided that the two components mix in a lateral way. In a recent experimental study of this three-component system it was demonstrated[7] that for the Pd_xCu_{1-x} alloy the CLSs of Cu $2p$ are different in two- and three-dimensions. Alloying takes place above 525 K and it is experimentally possible to distinguish between Pd $3d_{5/2}$ core electrons originating from atoms in the very surface and the subsurface layer(s). Pronounced changes in the valence band energy distribution curves (EDCs), both in the two-dimensional and the several layers thick films, are due to a strong mixing of the constituent Pd and Cu atoms. This conclusion is confirmed by recent

TABLE I. Characteristic experimental parameters for the substrate Ru(0001) and overlayer components Ag, Cu, and Pd.

Element	Lattice parameter (Å)	T_{d1} (K)	T_{d2} (K)	F (Ref. 11) (J/m^2)	Compounds (Ref. 10)	References metal/Ru
Ru	2.70			3.4		
Ag	2.89	1030 (Refs. 17 and 18)	890	1.1	$Ag_{1-x}Pd_x$	Ag/Ru (Refs. 12–16)
Cu	2.56	1220 (Ref. 9)	1130	1.9	CuPd, Cu_3Pd	Cu/Ru (Refs. 17–23)
Pd	2.75	1420 (Ref. 24)	1250	2.0		Pd/Ru (Refs. 14 and 24–27)

STM observations mentioned in Ref. 8. An extensive study of the conditions for surface alloying for Au—Ag on Ru(0001) as a substrate was made earlier by Bzowski *et al.*[9]

In the present report we investigate, theoretically and experimentally, the binding energy shifts in ultrathin films of pure Pd, Pd_xCu_{1-x}, and Pd_xAg_{1-x} on a Ru(0001) substrate in the thickness range from 1 to 4 ML for a variety of compositions of the surface alloys. The complete screening picture is used to calculate all the shifts. It is shown how the layer composition profile of a four-layer thick Pd_xAg_{1-x} film, formed by successive deposition of Ag and Pd on Ru(0001), and its evolution with increasing temperature can be followed by combining the theoretical modeling with experimentally determined Ag $3d_{5/2}$ CLSs and photoelectron intensities.

Concerning the lattice matching between the three metals, Ru, Pd, and Ag, then the Ag(111)-Ru(0001) faces have the highest mismatch, ~7%. In the submonolayer range, Pd forms pseudomorphic islands on Ru(0001), the Pd interatomic distances being isotropically compressed, whereas those of submonolayer Ag islands on Ru(0001) are only uniaxially compressed. Further, Ru has the highest and Ag the lowest surface energy. Also, it is well known[10] that Pd and Ag form alloys in the bulk, thus the mixing energy should not prevent mixing of Ag and Pd in films on Ru(0001). For the purpose of analysis and discussion a number of characteristic parameters for the substrate Ru(0001) and the overlayer components, Ag, Cu, and Pd, are collected in Table I. The parameters include the lattice parameter, the surface free energy, F, the desorption temperature of 1 ML, T_{d1}, multilayers, T_{d2}, and the stoichiometry of compounds according to the phase diagrams. References are given in the table and the ones with relevance to the morphology of the metal/Ru(0001) interfaces are given in the last column of the table.

The paper is organized as follows. In Sec. II the experimental conditions, primarily the parameters for the measurements of photoelectron spectra, are given. Section III introduces the theory behind the calculations of the layer-specific CLS. Results and discussion are collected in Sec. IV, with subsections for the different metal and surface alloy systems. Finally, conclusions are given in Sec. V.

II. EXPERIMENTAL

The experiments were performed at the storage ring, ASTRID, Aarhus University, at a beam line equipped with a spherical grating monochromator and a SCIENTA hemispherical concentric analyzer with a 20 cm radius and a channelplate as detector. Highly resolved $3d_{5/2}$ core-level spectra of Ru, Pd, and Ag were recorded with photon energies of 350, 400, and 437 eV, respectively, and a total instrumental resolution of better than 200, 250, and 300 meV, respectively. Cu $2p$ core electrons were excited with photons from a Mg K_α x-ray tube. The facilities of the endstation and the preparation of the Ru(0001) surface have been described in an earlier report.[7] The evaporation source was loaded with three metal samples, Ag, Cu, and Pd. Overlayers of Cu and Ag were prepared by evaporation from an electron bombarded crucible and Pd was evaporated from a tip of a thin Pd wire heated by direct electron bombardment. For the purpose of calibration a quartz crystal microbalance could be inserted in the line of sight between the respective evaporators and the Ru(0001) single crystal. Similar to the calibration of the Pd and Cu overlayers, based on recording of the $3d$ and $2p$ core-level spectra, respectively, the assessment of the 1 ML Ag coverage could be performed by measurement of the Ag $3d$ growth curve. Typically, the depositions were carried out with the Ru substrate kept at 550 K in order to prevent CO from sticking to Ru and Pd. Possible contaminations of the films with CO and O during the experiments were checked carefully by measuring the C $1s$ energy region and the valence band energy region from the Fermi edge to 15 eV binding energy. Possible presence of CO and/or O can easily be detected due to the energy positions of CO orbitals and O-$2p$. The time scale for the recording of the photoelectron spectra was kept below uptake of CO and/or O as judged from the nonpresence of any impurity signals in the energy intervals of relevance. The homogeneity and structures of the thin films were checked by recording of LEED patterns.

The analysis and fitting of the core level spectra were based on a Doniach-Sunjic line shape[28] convoluted with a Gaussian distribution.[29] Essential line-shape parameters are the asymmetry parameter α and the full width half maximum, Γ. One instance is the Ag $3d_{5/2}$ core-line spectrum for 1 ML Ag on the Ru(0001) substrate fitted at room temperature with $\Gamma=0.58$ eV and $\alpha=0.005$.

III. THEORY

First-principle calculations according to the complete screening picture are here used to determine the layer specific core-level binding energy shifts in the investigated metal and random surface alloys on Ru(0001). The complete screening picture was first used to calculate the CLS of an

atom in a metal, with the free atom as a reference,[30] and has thereafter been successfully applied for example for studies of CLS in disordered alloys[1,2] and at surfaces.[31–33] Recently the approach was extended to calculations of Auger kinetic energy shifts and applied to a study of the $L_3M_{45}M_{45}$ shift in fcc random PdAg alloys, with excellent agreement between the theory and experiment.[34] While there are many factors which can contribute to binding energy shifts, such as intra- and interatomic charge transfer, core hole relaxation, and the redistribution of charge due to bonding and hybridization,[35] all of these factors are incorporated into the complete screening picture, as the initial and final state effects are simultaneously included in a calculational scheme which only use the total energies of the studied systems.

The initial state contribution is readily given from the difference in electron energy eigenvalues referenced to the Fermi level and can be used as a first approximation to CLS. The final state effects are, however, not always negligible and may give a large contribution to the total shift, and even change its sign. The origin of the final-state effect is the relaxation in energy upon the presence of a core hole, which effectively acts as an extra proton and is screened by conduction charge as the core electron excites. The difference in relaxation is pronounced if the character of the screening charge is changed, e.g., from a *d* orbital in the reference system to an *sp* orbital in the studied material.

Our calculations use the generalized thermodynamic chemical potential (GTCP) of core-ionized atoms, μ, which corresponds to the ionization energy of a single core-electron,

$$\mu = \left.\frac{\partial E_{tot}}{\partial c}\right|_{c\to 0}. \quad (1)$$

E_{tot} is the total energy of a system with a concentration c of core-ionized atoms of an element. The fully screened core hole is modeled by promoting the ionized electron into the valence band. In addition to the initial state ($c=0\%$), computations are made for systems with $c=2\%$ ionized atoms. The BE shifts are in turn given by

$$\Delta_{X-ref} = \mu_i^X - \mu_i^{ref}; \quad (2)$$

here μ_i^X denotes the GTCP for a core level i in an atom situated at a specific layer X in the considered system. In other words the theoretical CLS, Δ_{X-ref}, is layer dependent, and GTCPs are obtained separately for each layer. As a reference in Eq. (2), μ_i^{ref}, we choose the GTCP obtained for 1 ML metal on Ru(0001), to make a direct connection with the presented experimental results.

All calculations are done within the density functional theory (DFT) and the local spin density approximation (LSDA)[36,37] with a parametrization of the one-electron exchange correlation potential and energy functional according to Perdew *et al.*[38] To calculate the GTCP in Eq. (1) we use the interface Green's function technique and the Korringa, Kohn and Rostocker method within the atomic sphere approximation (KKR-ASA),[39] in combination with the coherent potential approximation (CPA).[40,41] The basis set of *spd* muffin-tin orbitals was employed. For theoretical consistency only calculated Ru lattice parameters are used. The lattice parameter is fixed which means that no surface or local lattice relaxations are allowed. In earlier studies good theoretical results were obtained for the bulk CLS in fcc random PdCu and PdAg alloys.[1,2] Using the same computational methods as in the present work, Pd $3d_{5/2}$ layer-resolved CLSs for the systems Pd(100), 1 ML Mn/Pd(100), and three selected PdMn structures on Pd(100) were compared to experimental results. While the agreement with experiment was good for the Pd(100) and 1 ML Mn systems, the experimental PdMn structure could in addition be determined by a direct comparison between calculated and experimental CLSs.[31]

In the present work a number of different metal and surface alloys on Ru(0001) are investigated. This includes 1 ML Cu, Ag, and Pd, 2 ML and 4 ML Pd metals on Ru, as well as Pd_xCu_{1-x} and Pd_xAg_{1-x} surface alloys of different compositions and number of total layers on the Ru substrate. The studied systems on Ru(0001) are modeled as a continuation of the hcp(0001) stacking sequence *ABAB*…. In reality the overlayers can be stacked as *ABCABC*…, corresponding to the fcc structure of the corresponding bulk alloys [in (111) direction]. However, because of the similarity of the stackings, and rather small thickness of the overlayers, the difference in CLS calculated for the model and for the possible real surface structure is expected to be small in most of the cases. As a simple test of the structural dependence of the CLS, calculations were made for 4 ML uniformly random equiatomic PdAg alloys on Ru assuming hcp(0001) and fcc(111) structure for the whole system. A resulting variation in the layer-specific shifts was very small, between 3 and 20 meV.

IV. RESULTS AND DISCUSSION

A. Pd $3d_{5/2}$ CLS for Pd on Ru(0001)

In Table II the calculated, layer-resolved, CLS and SCLS for the proposed hcp structure of Pd on Ru(0001) are compared with the experimental results for two overlayer coverages, 2 and 4 ML Pd/Ru(0001). In the experiments,[7] distinct LEED patterns with well-focused spots were observed confirming the epitaxial growth of Pd on Ru(0001). The layer notation subML, IF, and S correspond to the submonolayer (coverage <1 ML), interface, and the surface components, respectively. For the 4 ML thick Pd film, the calculated CLSs of the Pd atoms, which are fully surrounded by Pd atoms, differ between the two "bulk" layers, which accordingly are denoted B_1 and B_2, with B_1 corresponding to the layer closer to the substrate. The differences in BEs demonstrate thin film, surface, and substrate effects on the Pd $3d_{5/2}$ core-level. Notice that a negative shift corresponds to a lower BE as compared to the reference.

The theoretical layer-specific shifts relative to 1 ML Pd/Ru(0001) are listed in the third column. The experimentally determined BEs are given in column 4. It is seen that the BE values for the subML differ slightly for the three films, which represent different experiments. The scattering reflects the experimental uncertainty, less than 20 meV. In column 5 follows the corresponding CLSs for the 1 ML case,

TABLE II. Calculated and experimental CLSs of Pd $3d_{5/2}$ are presented for 2 and 4 ML Pd/Ru(0001), using the 1 ML Pd/Ru(0001) as reference (Δ_{X-1}). The layers are denoted IF for the interface layer, B_1 and B_2 stand for the first and second layer from the IF layer, respectively; S is the surface layer. The experimentally determined BEs are given in the fourth column, including results for experimental coverages less than 1 ML (subML). The experimental reference BE to obtain CLS is the subML for 4 MLs. The energy unit is eV.

L_{tot}	Layer	Theory Δ_{X-1}	Experiment BE (Ref. 7)	Δ_{X-1}
1	subML		335.08	
2	subML		335.09	
	S	−0.37	334.74	−0.32
	IF	0.23	335.27	0.21
4	subML		335.06	
	S	−0.43	334.74[a]	−0.32
	B_2	−0.19	334.84	−0.22
	B_1	−0.11		
	IF	0.27	335.27[a]	0.21

[a]The BEs for the 4 ML components S and IF are kept fixed from the 2 MLs thick film.

Δ_{X-1}. As reference BE the subML from 4 MLs is used. Thus a direct comparison can be made between the calculated CLS and the experimental results.

1. Comments on 2 ML Pd/Ru(0001)

The experimental BE values are determined from the decomposition of the Pd $3d_{5/2}$ energy distribution curve (EDC) for a 2 ML thick Pd film[7] in two components with BE(S) =334.74 eV and BE(IF)=335.27 eV. The theoretically determined SCLS, for S, relative to the subML component, is in good agreement with the experimental value. The difference is only 51 meV. Experimentally the shift between the S and IF components, Δ_{IF-S}=0.53 eV, is slightly lower than the corresponding theoretical value, 0.60 eV. Finally, the theoretically determined shift of the IF component, Δ_{IF-1} =0.23 eV, lies inside the range of the experimentally found value, taking the uncertainty into consideration. It is concluded that there is a very good agreement between the calculated and experimentally determined core level shifts for the 2 ML Pd/Ru(0001) interface.

2. Comments on 4 ML Pd/Ru(0001)

The BEs listed in Table II, column 4, are determined by fitting of the Pd $3d_{5/2}$ spectrum published in Ref. 7 with the experimentally found shifts Δ_{S-1}=−0.32 eV and Δ_{IF-1} =0.21 eV between the subML and the S and IF components (see Table II), respectively. Theoretically (Table II), the B_1 and B_2 shifts were found to be −0.11 and −0.19 eV, respectively. From thickness considerations it is expected that the B_2 component will dominate the collective bulk contribution to the measured spectrum from a four-layer Pd film due to the attenuation caused by the overlayers. The experimentally found value of the "bulk" shift relative to the subML component is −0.22 eV, which deviates 0.04 eV from the dominant B_2 value. Similar for the S component, a 0.11 eV deviation between theory and experiment is found. A reasonable agreement between theory and experiment for the Pd $3d_{5/2}$ CLS in a four-layer thick Pd film on Ru(0001) is obtained. It should be noted that the signs of the shifts from the different layers are reproduced.

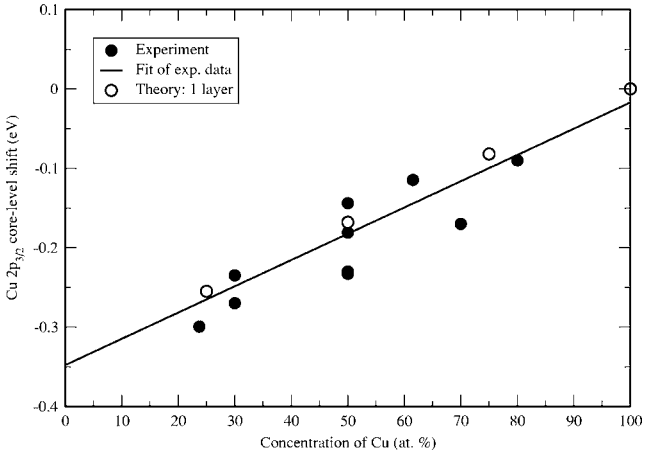

FIG. 1. Theoretically and experimentally determined Cu $2p_{3/2}$ core-level shifts as a function of the composition of the bimetallic alloy Pd_xCu_{1-x} in two dimensions, a single overlayer on the template Ru(0001). The composition of the two-dimensional surface alloy is expressed by at. % Cu. The total coverage of Cu and Pd is 1 ML and the overlayers have been annealed to 1000 K. The theoretical results are indicated with an open square and the experimental points are indicated as filled circles. As reference for CLS the Cu $2p_{3/2}$ BE for 1 ML Cu is chosen. The full drawn line represents the best linear fit to the experimental points.

B. Cu $2p_{3/2}$ CLS in two- and three-dimensional Pd_xCu_{1-x}/Ru(0001)

In this section the possibility of investigating an Pd_xCu_{1-x} alloy in two and three dimensions by means of SCLS and CLS, both theoretically and experimentally, is demonstrated. The experimentally determined correlations between the core-level shifts of Cu $2p_{3/2}$ and the compositions of the Pd_xCu_{1-x} alloys in two and three dimensions are displayed in Figs. 1 and 2, respectively. As a reference energy the BE of 1 ML of Cu on Ru(0001) is chosen. That is, the reference value for the experimentally found BEs is the (constant) BE measured for 0–1 ML Cu coverage on Ru(0001).[17,22] The overlayers were annealed at 1000 K before measurements. Correspondingly, the theoretical CLS is referenced to 1 ML Cu/Ru(0001). Since the graphs involve two experimentally determined coordinates, there is an uncertainty regarding the ordinate around 25 meV, and an estimated accuracy of 0.05 on the stoichiometry. There is a very good agreement between theory and experiment in the two-dimensional case as shown in Fig. 1. Assuming a linear relation between Δ_{S-1} and the atomic concentration of Cu, both theory and experiments give an inclination equal to 0.34 eV/unit concentration.

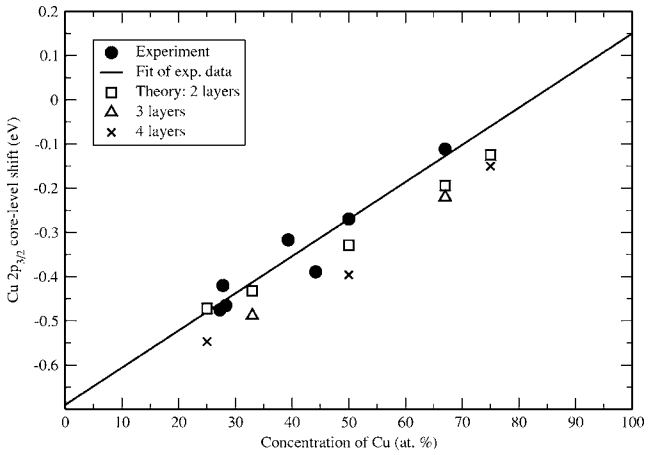

FIG. 2. Theoretically and experimentally determined Cu $2p_{3/2}$ core-level shifts, as a function of the composition of the bimetallic alloy Pd_xCu_{1-x} in three dimensions. The three-dimensional bimetallic overlayers, with total coverages above 1 ML, were annealed at 765 K. Theoretical CLSs Δ_{S-1} from 2 to 4 ML systems are indicated as open squares, open triangles, and "x," respectively; the experimental points are shown as filled circles. The full drawn line represents the best linear fit to the experimental points.

Keeping the same reference level, 1 ML Cu/Ru(0001), the experimental and calculated shifts are shown in Fig. 2 for the three-dimensional Pd_xCu_{1-x} alloys. These overlayers were annealed at 765 K. A series of LEED patterns demonstrating the homogeneity and structure of the Pd_xCu_{1-x} alloys was published recently in Ref. 7. The experimental Cu $2p_{3/2}$ BE shifts are measured from 2–4 ML thick films. Due to the mean free path of the photoelectrons the measurements record two or several layers. The same linear relation, having an inclination of 0.840 eV/unit concentration, fits all experimental points. The theoretical values displayed in Fig. 2 are calculated assuming homogeneous concentration profiles (which is not necessarily the case in experiment) and represent the Cu $2p_{3/2}$ BE shift of Cu atoms at the surface of different alloys. The overlayer thickness is varied from two to four layers. Again good agreement is observed between theoretical and experimental values. It should be noted that theoretical calculations (not shown in Fig. 2) indicate that the shifts for Cu atoms at the interface are similar to the two-dimensional case, while the layers between the surface and the interface are smaller than, though closer to, Δ_{S-1} for the Cu atoms in the surface layer. From Figs. 1 and 2 the following derivative ratios for the linear correlations are read: the theoretical derivative ratio, $f_{th}=\alpha_3/\alpha_2=0.695/0.345=2.0$, with α_3 from 2 ML systems, and the experimental derivative ratio, $f_{ex}=0.840/0.331=2.5$. It is concluded that (*i*) there exists, to a good approximation, a linear relationship between Cu $2p_{3/2}$ binding energy shifts and the Cu concentration in both two- and three-dimensional Pd_xCu_{1-x} surface alloys and (*ii*) there is a very good agreement between theory and experiment.

C. Pd $3d_{5/2}$ CLS in Pd_xCu_{1-x}/Ru(0001)

A direct comparison between theory and experiment[7] for Pd $3d_{5/2}$ CLSs can be performed for a two-layer thick, mixed, $Pd_{50}Cu_{50}$ film deposited at 550 K with Cu as the first deposit. The same spectrum is observed after annealing to 1000 K.[7] There are only two different Pd components in the film, one from the surface with a BE=334.81 eV and one from the interface layer with BE=335.42 eV. Thus, the Pd $3d_{5/2}$ BE difference Δ_{IF-S} can be studied. The experimentally determined shift, 0.61 eV, is in excellent agreement with the result from the complete screening picture, 0.62 eV. As presented in Ref. 7 the same experimental value is found for the

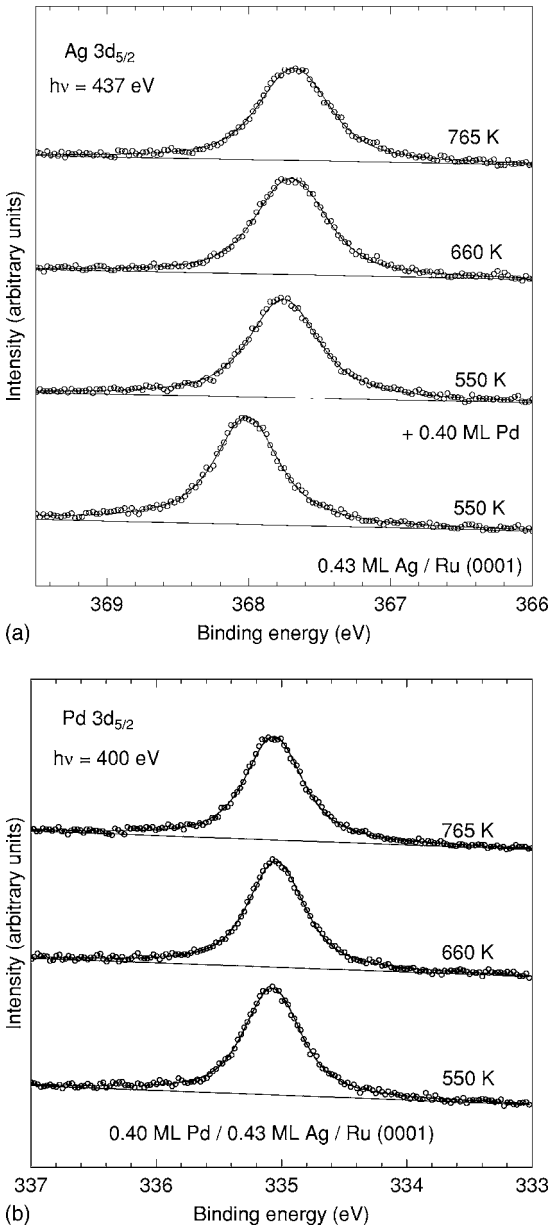

FIG. 3. (a) Left column shows Ag $3d_{5/2}$ PES spectra. The lower spectrum represents a 0.43 ML Ag/Ru(0001) interface, with Ag deposited at a temperature of 550 K, recorded for a photon energy of 437 eV. Subsequently 0.40 ML Pd was deposited at 550 K. The following spectra represent the same interface after annealings for 5 min at the temperatures indicated, 660 K and 765 K. (b) Corresponding Pd $3d_{5/2}$ PES spectra from the 0.40 ML Pd/0.43 ML Ag/Ru(0001) interface recorded for a photon energy of 400 eV, lower spectrum, and subsequently annealed at 660 K and 765 K.

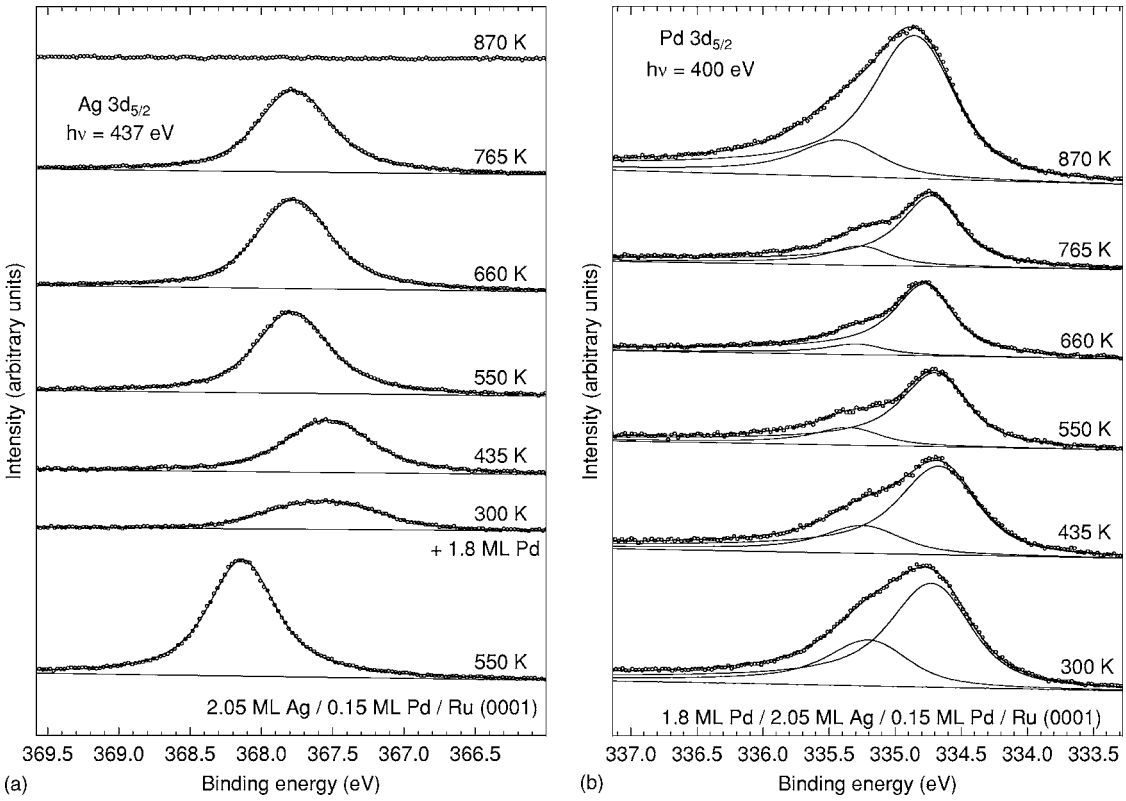

FIG. 4. (a) Left column: Ag $3d_{5/2}$ PES spectrum recorded for a photon energy of 437 eV from 2.05 ML Ag deposited on 0.15 ML Pd/Ru(0001) surface at 550 K, lower spectrum. The next spectrum is recorded after deposition of 1.8 ML Pd at room temperature. They subsequently represent the same spectrum after annealing at the given temperatures. At 870 K Ag has desorbed. (b) Corresponding Pd $3d_{5/2}$ PES spectra taken with a photon energy of 400 eV. Fitting curves, representing contributions from surface and subsurface components, are shown for 2.2 ML Pd and for the alloy at $T>550$ K.

opposite sequence of deposition, Pd before Cu, followed by annealing at 660 K.

D. Pd and Ag $3d_{5/2}$ CLS in Pd_xAg_{1-x}/Ru(0001)

In the present experiments it was found that the growth of Ag on Ru(0001) at 550 K is characterized by a constant BE=367.91 eV for Ag $3d_{5/2}$ for coverages below 1 ML, followed by an increase of 0.14±0.10 eV at a coverage of 2 ML.

Two different depositions of Pd and Ag on Ru(0001) at 550 K were performed with total coverages representing 0.83 and 4.0 ML. EDCs of the $3d_{5/2}$ core electrons from Ag and Pd for the total coverage of 0.83 ML are shown in Figs. 3(a) and 3(b), recorded for photon energies of 437 and 400 eV, respectively. Deposition of 0.40 ML Pd on the 0.43 ML Ag/Ru(0001) interface at 550 K causes, see Fig. 3(a), a decrease of −0.25 eV in the BE of Ag $3d_{5/2}$ and a small reduction, 6%, of the intensity. The last observation indicates a planar distribution of the two metals. The FWHM increase of Ag $3d_{5/2}$ after deposition of 0.40 ML Pd is ascribed to core level disorder broadening in agreement with the observation and interpretation of core photoelectron linewidth broadening in AgPd alloys.[42] The evolution of the spectra with succesive annealings to 765 K is characterized by (*i*) a very small negative BE shift, −50 meV, and a 8% intensity decrease of the Ag $3d_{5/2}$ electrons and (*ii*) no changes in the BE and intensity of the Pd $3d_{5/2}$ electrons. Thus, the bimetallic two-dimensional PdAg overlayer, formed at 550 K, is stable at higher temperatures; a conclusion which is confirmed by the constancy of the valence band EDCs.[43] By applying the complete screening picture described in Sec. III to an ideal system 1 ML $Ag_{50}Pd_{50}$/Ru(0001), the corresponding theoretical shifts are −0.20 eV for Ag and 0.04 eV for Pd, which agree very well with experiment (−0.25 and 0.00 eV, respectively).

Ag and Pd $3d_{5/2}$ EDCs obtained for a 4 ML film are shown in Figs. 4(a) and 4(b). The lowest spectrum in Fig. 4(a) represents a 2.05 ML thick Ag overlayer, deposited at 550 K, on Ru(0001) with a residual Pd coverage estimated to be 0.15 ML. A LEED pattern, Fig. 5(a), for this film is taken for normal incidence and with a primary electron beam energy of 115 eV. A hexagonal structure is observed. Deposition of 1.8 ML Pd at 300 K results in a Ag $3d_{5/2}$ negative BE shift, −0.43 eV, and a strong reduction of the peak intensity to 25%. As demonstrated in the LEED pattern, Fig. 5(b), recorded for a primary beam energy of 148 eV, the film still exhibits a hexagonal pattern. According to the valence band spectra there is a weak interdiffusion between the layers even at this temperature. Taking the penetration depth into consideration, roughly three atomic layers, and assuming homogeneity in these layers, the above-measured BE shift corresponds to a 20% Ag concentration in the top layers. Pd is lying on top of the two Ag layers with a smaller amount of

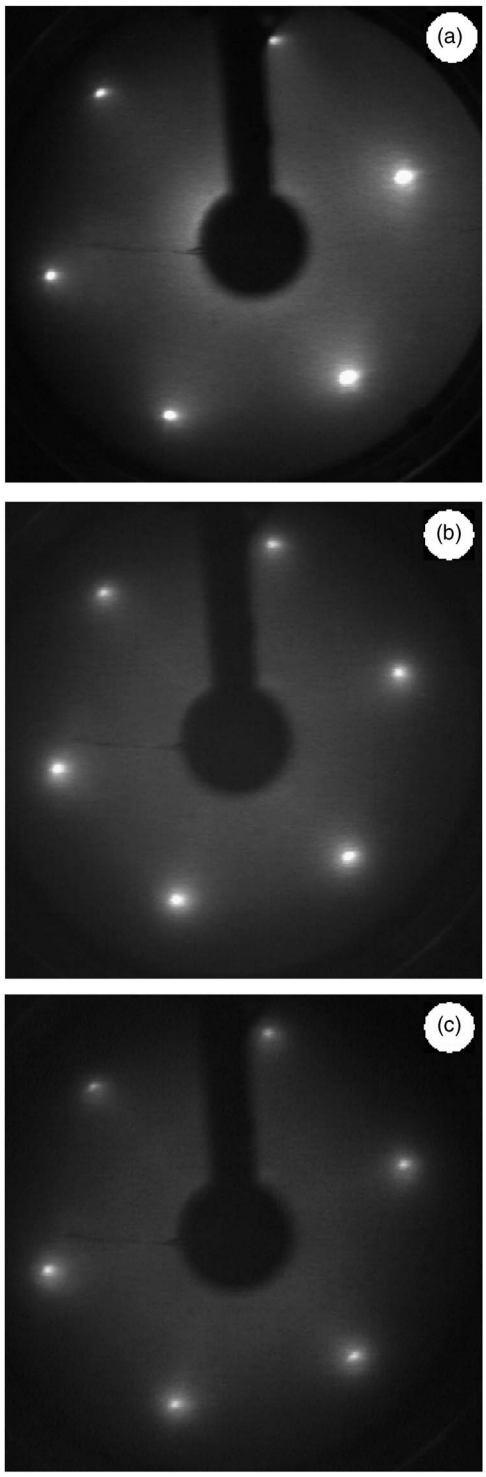

FIG. 5. LEED patterns for normally incident primary electrons of energy Ep, (a) 2.05 ML Ag deposited on 0.15 ML Pd/Ru(0001) at 550 K, $Ep=115$ eV; (b) 1.8 ML Pd+2.05 ML Ag on Ru(0001), Pd deposited at 300 K, $Ep=148$ eV; and (c) the last overlayer after annealing at 550 K for 5 min, $Ep=148$ eV.

interdiffusion. Also, the Ag $3d_{5/2}$ feature is very broad with a full width half maximum (FWHM) equal to 0.9 eV. These observations show that a sandwich consisting of ~2 ML Ag with ~2 ML of Pd, with some mixing, is formed. The reason for the large Ag $3d_{5/2}$ CLS after deposition of Pd is found in the Ag positioned at the interface and a pronounced change in the centroid of the Ag $4d$ valence electron distribution.[43] The large FWHM is ascribed to the distribution of Ag over several layers and types of sites.

1. Evolution of the **Pd+Ag** *sandwich with temperature*

Annealing at 435 K for 5 min results in a 60% increase of the Ag intensity, an unchanged BE, and a 12% reduction of the total FWHM. These changes are ascribed to enhanced diffusion of Ag into the two uppermost layers. Further annealing at 550 K causes a segregation of Ag to the surface, a 220 meV increase of the Ag $3d_{5/2}$ BE to 367.78 eV, a reduction of the FWHM to 0.6 eV, and an increase of the Ag intensity with 100%. A reorganization of the PdAg sandwich takes place. The structure of the four-layers thick film is conserved as demonstrated in the LEED patterns, Fig. 5(c), with $Ep=148$ eV. The film composition remains at a temperature of 765 K. Complete removal of Ag is observed at a temperature of 870 K. This evolution with temperature is mirrored in the Pd $3d_{5/2}$ EDCs, Fig. 4(b), with a 60% intensity reduction from the initial state at 300 K to the minimum intensity at 660 K, changes in the intensity balance between the high- and low-BE parts of the Pd feature, and 35% variation of the FWHM over the temperature interval. The drawn curves are the results of fitting with two peaks with equal Gaussian widths and the following constants: Lorentzian width LW=0.4 eV and $\alpha=0.11$. Based on the EDCs in Figs. 3 and 4 experimental CLS can be determined. The results obtained from the 4 ML experiment are collected in the case of Ag $3d_{5/2}$ in Table III and for Pd $3d_{5/2}$ in Table IV together with the layer-resolved theoretical CLSs for different concentration profiles for a 4 ML equiatomic PdAg system on the Ru substrate. The content and results presented in Table III and IV are discussed in the following two subsections.

2. Comments on Ag $3d_{5/2}$ *CLS*

The experimental information is, besides the CLSs, the intensity changes of Ag $3d_{5/2}$ and Pd $3d_{5/2}$, and the FWHMs. It should be added that, with the chosen photon energies, the information depth is limited to roughly 3 ML with an exponential decaying intensity from the surface layer to the third layer. Another constraint in comparison between experiment and theory includes the "single peak" structure of the observed Ag $3d_{5/2}$ spectrum, which represents mainly an overlap of two to three components from the upper layers while the theoretical modeling gives CLSs for the individual layers. The theoretical shifts are also derived from four complete layers with a total equiatomic concentration of Ag and Pd.

The results compiled in Table III start with the initial system of 2 ML Ag with the residual 0.15 ML Pd. Note that the theoretical shifts in the concentration profile containing Pd is closer to the experimental value compared to the case of 2 pure ML Ag. In Table III six different composition profiles a–f are considered for the 4 ML system. Based on the intensity evaluations and the VB density of states,[43] the first composition profiles are chosen as dominated by Pd in the top two layers with a substantial amount of Ag. Profile a

TABLE III. Calculated and experimental CLSs of Ag $3d_{5/2}$ for 2 and 4 ML PdAg systems on Ru referenced to 1 ML Ag/Ru(0001), Δ_{X-1}. The layers are denoted as in Table II. Experimental BEs are given for specific annealing temperatures with corresponding shifts. Theoretical layer resolved shifts of Ag are given for concentration profiles ($S:B_2:B_1:IF$) a–f for 4 ML equiatomic PdAg-systems, the same as in Table IV. The concentration profiles corresponding to the 2 ML system are given explicitly in the table in terms of at. % Pd (S:IF). The energy unit is eV.

L_{tot}	Layer	Theory Δ_{X-1}						Experiment BE	Δ_{X-1}	
2		(0:0)	(0:15)					$T=550$ K		
	S	0.22	0.18					368.14	0.14	
	IF	0.30	0.23							
4		Profile[a]	Profile[b]	Profile[c]	Profile[d]	Profile[e]	Profile[f]	$T=300$ K		$T=550$ K
	S		−0.57	−0.40	−0.20	−0.12	−0.03	367.57	−0.43	−0.21
	B_2	−0.43	−0.43	−0.28	−0.15	−0.10	−0.04			
	B_1	0.00	−0.18	−0.23	−0.27	−0.29	−0.30			
	IF	0.13	0.02	−0.12	−0.20	−0.23	−0.25			

[a]Concentration profile ($S:B_2:B_1:IF$); Pd: $Pd_{85}Ag_{15}:Ag:Pd_{15}Ag_{85}$, (100:85:0:15).
[b]$Pd_{80}Ag_{20}:Pd_{60}Ag_{40}:Pd_{50}Ag_{50}:Pd_{10}Ag_{90}$ (80:60:50:10).
[c]$Pd_{50}Ag_{50}$, (50:50:50:50).
[d](30:40:60:70).
[e](20:40:60:80).
[f](10:40:60:90).

corresponds to the case that the deposited Pd stays on top with no intermixing with Ag, while in profile b Pd dominates on the surface, with some mixing of Ag. Profile c represents the ideal homogeneous case with $Pd_{50}Ag_{50}$ in every layer and is given as a reference for the other concentration profiles. Finally, in the 550 K annealed state, the Ag dominance in the S and B_2 layers roughly corresponds to the concentration profile d with a 70% and 60% Ag dominance, in the respective layers. In profiles e and f the amount of Ag has increased and is dominating in the surface and near-surface region, S and B_2. It is interesting to compare the two distinct Ag $3d_{5/2}$ CLSs observed in Fig. 4(a) with theory. The Δ_{X-1}^{exp} shifts amount to (*i*) −0.43 eV when 2 ML Pd is deposited and to (*ii*) −0.21 eV when the PdAg sandwich is annealed at 550 K, an increase of +0.22 eV. The theoretical calculations show a similar trend upon increasing the amount of Ag at the surface.

In order to provide an additional basis for comparisons between theoretical and experimental results for the four-layer thick film, core-level spectra have been modeled on the basis of a template spectrum, the calculated CLSs, a reasonable choice of attenuation coefficient, and then compared with the experimental spectra. In the following paragraphs, the model is outlined and the results are displayed in Figs. 6 and 7 together with the original measured spectra.

First, a template spectrum representing a fit of the line shape and BE to an experimental photoelectron spectrum from one complete layer of Ag $3d_{5/2}$ is generated. A resulting

TABLE IV. Calculated and experimental CLSs of Pd $3d_{5/2}$ for 4 ML PdAg systems on Ru referenced to 1 ML Pd/Ru(0001), Δ_{X-1}. The layers are denoted as in Tables II and III. Experimental BEs are given for specific annealing temperatures with corresponding shifts. Theoretical layer resolved shifts of Pd are given for different concentration profiles a–f defined in Table III for 4 ML equiatomic PdAg-systems. Table III displays the corresponding results for Ag. The energy unit is eV.

L_{tot}	Layer	Theory Δ_{X-1} Profile[a]	Profile[b]	Profile[c]	Profile[d]	Profile[e]	Profile[f]	Experiment BE $T=300$ K	Δ_{X-1}	$T=435$ K	$T=660$ K
4	S	−0.45	−0.44	−0.44	−0.34	−0.29	−0.23	334.70	−0.36	−0.41	−0.31
	B_2	−0.16	−0.22	−0.17	−0.11	−0.06	−0.02	335.17	0.11		
	B_1		−0.06	−0.08	−0.07	−0.07	−0.07				
	IF	0.38	0.32	0.29	0.28	0.28	0.28				

[a]Concentration profile ($S:B_2:B_1:IF$); Pd: $Pd_{85}Ag_{15}:Ag:Pd_{15}Ag_{85}$, (100:85:0:15).
[b](80:60:50:10).
[c](50:50:50:50).
[d](30:40:60:70).
[e](20:40:60:80).
[f](10:40:60:90).

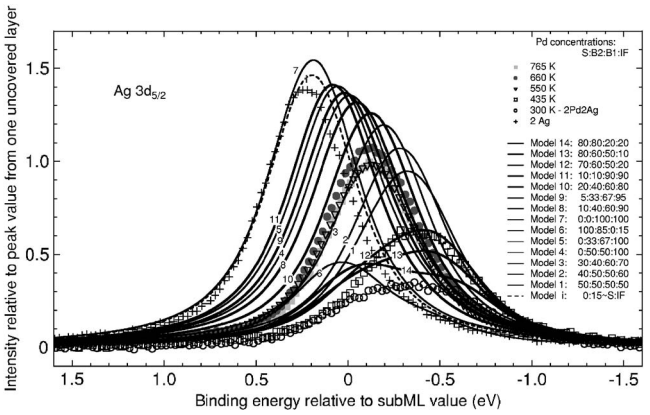

FIG. 6. Model (full lines) and experimentally recorded (separate points) Ag $3d_{5/2}$ core-level spectra for 4 MLs of Pd and Ag deposited on Ru(0001). The experimental spectra are identical to the ones shown in Fig. 4(a). The Pd concentration profiles, in all 15 different model cases, for the four bimetallic overlayers are listed to the right in the figure.

Ag $3d_{5/2}$ template spectrum, derived from a spectrum measured at an interface with a coverage of 0.9 ML Ag on Ru(0001), has the following line-shape parameters: FWHM $=0.58$ eV and $\alpha=0.005$. The corresponding parameters for Pd are FWHM$=0.60$ eV and $\alpha=0.07$. Hence, their widths are comparable, but where the Pd template spectrum exhibits an appreciable asymmetry, the one of Ag $3d_{5/2}$ is practically symmetric. With kinetic energies of 65 eV, an attenuation length, λ, corresponding to 1.7 layers is chosen that gives rise to a 55% attenuation of a signal from a certain layer for each layer it passes through. Next, the signal is scaled down with a factor according to the relative amount of atoms present in the layer, and, finally, the signal is shifted Δ_{X-1} along the BE axis in accordance with the results of the CPA calculations. The generation of a model spectrum is complete by summarizing the contributions from the respective layers.

Model Ag $3d_{5/2}$ spectra are displayed in Fig. 6, where the intensity relative to the intensity from one uncovered Ag layer is plotted as a function of BE. The five experimental spectra are compared with a span of model spectra with at. % Pd concentrations in the $S:B_2:B_1:IF$ layers listed to the right in the figure. It is seen that the 2 ML Ag spectrum is well reproduced by a model spectrum with 100% and 85% Ag in the S and IF layers, respectively. Interesting enough, the addition of 2 ML Pd at 300 K is well reproduced, both in terms of the large BE shift and the intensity, by model spectrum "13," consisting of the Pd concentrations: 80:60:50:10 (b in Table III). Thus, the model confirms a smaller diffusion of Ag in the top layers. The evolution of the spectrum with increasing annealing temperatures, characterized by the three close-lying experimental spectra in the temperature range 550–765 K, is reproduced in model spectrum "10" where the Pd concentrations in the four layers are 20:40:60:80 (e in Table III). The above-mentioned observed two distinct Ag $3d_{5/2}$ CLSs, −0.43 and −0.21 eV, can thus be accounted for in a satisfactory way. Thus a model based on an experimentally determined template Ag $3d_{5/2}$ spectrum and an attenuation coefficient with theoretically determined CLSs gives information on the composition of the individual layers and the evolution of the four-layer thick, mixed film with temperature. These trends are in accordance with the calculated CLS for Ag $3d_{5/2}$ in random Pd—Ag alloys.[2]

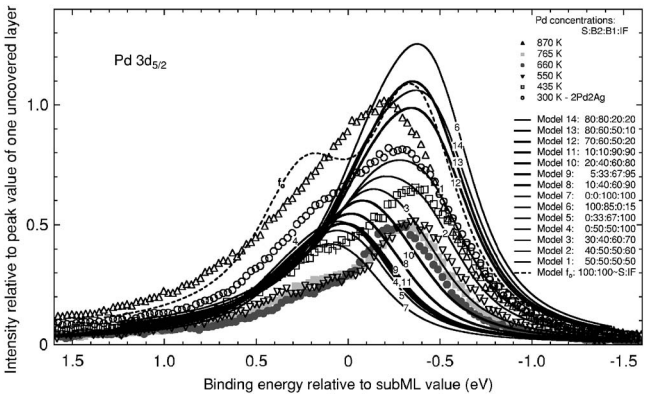

FIG. 7. Model (full lines) and experimentally recorded (separate points) Pd $3d_{5/2}$ core-level spectra for 4 MLs of Pd and Ag deposited on Ru(0001). The experimental spectra are identical to the ones shown in Fig. 4(b). The Pd concentration profiles, in all 15 different model cases, for the four bimetallic overlayers are listed to the right in the figure.

3. Comments on Pd $3d_{5/2}$ CLS

As mentioned before, the BE=335.06 eV is used as the constant for Pd $3d_{5/2}$ in the submonolayer range on Ru(0001) and this value is also found for the 0.40 ML Pd+0.43 ML Ag/Ru(0001) interface. As demonstrated in Fig. 4(b), the Pd structure for the 4.1 ML case at 300 K can be resolved into two peaks with a dominant intensity of the component at BE=334.70 eV and a low-intensity component at BE =335.17 eV. The low-BE peak is assigned as the surface peak and the high-BE peak is the subsurface peak. From these values the relative shift Δ_{X-S} is determined to 0.47 eV. The corresponding results for Pd $3d_{5/2}$ for the different concentration profiles a–f are collected in Table IV. Note that changes of the CLS at Pd atoms between different profiles are substantially smaller than in the case of Ag. As a matter of fact, this is in agreement with experiment, and it also corresponds to a weaker concentration dependence of Pd CLS, as compared to Ag, in bulk Ag—Pd alloys.[2]

Concerning the Pd $3d_{5/2}$ spectra, see Fig. 7, then the BE-shifts of the peak maxima are comparatively much smaller than in the case of Ag $3d_{5/2}$. The simplest spectrum is the one of the final state after annealing at 870 K where Ag has desorbed and only 2 ML of Pd is present. Two peaks, representing the S and IF peaks, are distinguishable in the model spectrum "f_0," that reasonably fits the measured spectrum. From a consistency point of view the earlier found best model spectra in the case of Ag $3d_{5/2}$, with the layer specific concentrations of Pd, should be applicable to the Pd spectra. It means that the model spectrum "10" should fit the three close-lying experimental Pd spectra in the range 550–765 K. As observed in Fig. 7, however, only the high-BE side is reproduced in the model spectrum while the low-BE contributions have too strong intensities with the consequence that the peak maximum is shifted −200 meV. In the modeling of

the Pd spectra several not included factors may cause the deviations between the model spectra and the measured spectra. Possible diffraction effects that modify the relative contributions from each layer are not considered. Another factor is that the submonolayer-like line shape used as the contribution from each layer might be a not adequate approximation since the Pd density of states close to the Fermi level is sensitive to the composition of the alloy.

V. CONCLUSIONS

First-principle calculations of layer specific core-level and surface core-level binding energy shifts in metal Pd, Ag, and surface alloy thin films Pd_xCu_{1-x} and Pd_xAg_{1-x} on Ru(0001) have been performed and compared with experimental values of the same films. There is a good agreement between the complete screening picture and experiments. Further, it was demonstrated that CLS and SCLS can be used as indicators for the composition of the alloys and calculated shifts follow the trend as the overlayers are annealed at different temperatures. The dimensionality effect observed in the Cu $2p_{3/2}$ CLS for two- and three-dimensional Pd—Cu random alloys over the compositions is closely reproduced in the calculations. The Cu SCLSs for the three-dimensional Pd_xCu_{1-x} alloy are twice as big as the shifts for the two-dimensional alloy, with the same stoichiometry, due to the different coordination numbers.

The layer composition profile of a four-layer thick Pd—Ag film, formed by successive deposition of Ag and Pd on Ru(0001), and its evolution with temperature, was determined by generation of model spectra that are compared with the experimental spectra. The best agreement is obtained for Ag $3d_{5/2}$.

ACKNOWLEDGMENTS

This work was supported by the Danish Natural Science Council. W.O., I.A.A., and B.J. are grateful to the Swedish Research Council (VR) and the Swedish Foundation for Strategic Research (SSF) for financial support. Part of the calculations were performed on Monolith cluster at the National Supercomputer Centre (NSC) in Linköping, Sweden.

[1] W. Olovsson, I. A. Abrikosov, and B. Johansson, J. Electron Spectrosc. Relat. Phenom. **127**, 65 (2002).
[2] I. A. Abrikosov, W. Olovsson, and B. Johansson, Phys. Rev. Lett. **87**, 176403 (2001).
[3] R. J. Cole, N. J. Brooks, and P. Weightman, Phys. Rev. Lett. **78**, 3777 (1997).
[4] R. J. Cole, N. J. Brooks, and P. Weightman, Phys. Rev. B **56**, 12178 (1997).
[5] N. Mårtensson, R. Nyholm, H. Calén, J. Hedman, and B. Johansson, Phys. Rev. B **24**, 1725 (1981).
[6] P. Steiner and S. Hüfner, Acta Metall. **29**, 1885 (1981).
[7] T. H. Andersen, L. Bech, Z. Li, S. V. Hoffmann, and J. Onsgaard, Surf. Sci. **559**, 111 (2004).
[8] T. Hager, H. Rauscher, and R. J. Behm, Surf. Sci. **558**, 181 (2004).
[9] A. Bzowski, M. Kuhn, T. K. Sham, J. A. Rodriquez, and J. Hrbek, Phys. Rev. B **59**, 13379 (1999).
[10] T. B. Massalski, *Binary Alloy Phase Diagrams*, 2nd ed. (ASM International, Materials Park, OH, 1990), Vol. 2.
[11] L. Z. Mezey and J. Geber, Jpn. J. Appl. Phys., Part 1 **21**, 1565 (1982).
[12] J. W. Niemantsverdriet, P. Dolle, K. Markert, and K. Wandelt, J. Vac. Sci. Technol. A **5**(4), 875 (1987).
[13] J. A. Rodriguez, Surf. Sci. **296**, 149 (1993).
[14] C. Park, Surf. Sci. **203**, 395 (1988).
[15] J. L. Stevens and R. Q. Hwang, Phys. Rev. Lett. **74**, 2078 (1995).
[16] R. Q. Hwang, J. C. Hamilton, J. L. Stevens, and S. M. Foiles, Phys. Rev. Lett. **75**, 4242 (1995).
[17] J. A. Rodriguez, R. A. Campbell, and D. W. Goodman, J. Phys. Chem. **95**, 2477 (1991).
[18] G. O. Potschke and R. J. Behm, Phys. Rev. B **44**, 1442 (1991).
[19] C. Günther, J. Vrijmoeth, R. Q. Hwang, and R. J. Behm, Phys. Rev. Lett. **74**, 754 (1995).
[20] K. Meinel, H. Wolter, C. Ammer, and H. Neddermeyer, Surf. Sci. **401**, 434 (1998).
[21] S. D. Ruebush, R. E. Couch, S. Thevuthsan, and C. S. Fadley, Surf. Sci. **421**, 205 (1999).
[22] T. H. Andersen, L. Bech, J. Onsgaard, S. V. Hoffmann, and Z. Li, Surf. Rev. Lett. **9**, 723 (2002).
[23] K. R. Zavadil, D. Ingersoll, and J. W. Rogers, Jr., J. Electroanal. Chem. **318**, 223 (1991).
[24] R. A. Campbell, J. A. Rodriguez, and D. W. Goodman, Phys. Rev. B **46**, 7077 (1992).
[25] S. Surnev, M. Sock, M. G. Ramsey, F. P. Netzer, M. Wiklunf, M. Borg, and J. N. Andersen, Surf. Sci. **470**, 171 (2000).
[26] T. H. Andersen, Z. Li, S. V. Hoffmann, L. Bech, and J. Onsgaard, J. Phys.: Condens. Matter **14**, 7853 (2002).
[27] R. Wu and A. J. Freeman, Phys. Rev. B **52**, 12419 (1995).
[28] S. Doniach and M. Sunjic, J. Phys. C **3**, 285 (1970).
[29] D. Adams (2001), the program FitXPS, unpublished.
[30] B. Johansson and N. Mårtensson, Phys. Rev. B **21**, 4427 (1980).
[31] W. Olovsson, E. Holmström, A. Sandell, and I. A. Abrikosov, Phys. Rev. B **68**, 045411 (2003).
[32] M. Aldén, H. L. Skriver, and B. Johansson, Phys. Rev. Lett. **71**, 2449 (1993).
[33] M. Aldén, I. A. Abrikosov, B. Johansson, N. M. Rosengaard, and H. L. Skriver, Phys. Rev. B **50**, 5131 (1994).
[34] W. Olovsson, I. A. Abrikosov, B. Johansson, A. Newton, R. J. Cole, and P. Weightman, Phys. Rev. Lett. **92**, 226406 (2004).
[35] M. Weinert and R. E. Watson, Phys. Rev. B **51**, 17168 (1995).
[36] P. Hohenberg and W. Kohn, Phys. Rev. **136**, B864 (1964).
[37] W. Kohn and L. J. Sham, Phys. Rev. **140**, A1133 (1965).
[38] J. P. Perdew, K. Burke, and M. Ernzerhof, Phys. Rev. Lett. **77**, 3865 (1996).
[39] H. L. Skriver and N. M. Rosengaard, Phys. Rev. B **43**, 9538 (1991).

[40] I. A. Abrikosov and H. L. Skriver, Phys. Rev. B **47**, 16532 (1993).

[41] A. V. Ruban and H. L. Skriver, Comput. Mater. Sci. **15**, 119 (1999).

[42] A. W. Newton, S. Haines, P. Weightman, and R. J. Cole, J. Electron Spectrosc. Relat. Phenom. **136**, 235 (2004).

[43] Energy distribution curve for the valence band density of states not shown here (unpublished).